

Article

Feedback and Feedforward Control of a Biotrickling Filter for H₂S Desulfurization with Nitrite as Electron Acceptor

Javier Brito , Fernando Almenglo , Martín Ramírez *  and Domingo Cantero

Department of Chemical Engineering and Food Technologies, Faculty of Sciences, University of Cadiz, Instituto Universitario de Investigación Vitivinícola y Agroalimentario (IVAGRO), 11510 Puerto Real, Cádiz, Spain

* Correspondence: martin.ramirez@uca.es; Tel.: +34-956-01-6286

Received: 26 April 2019; Accepted: 27 June 2019; Published: 30 June 2019



Abstract: Biotrickling filters' control for H₂S removal has special challenges because of complexity of the systems. Feedback and feedforward control were implemented in an anoxic biotrickling filter, operated in co-current flow mode and using nitrite as an electron acceptor. The feedback controller was tuned by three methods—two based on Ziegler-Nichols' rules (step-response and maintained oscillation) and the third using the Approximate M-constrained Integral Gain Optimization (AMIGO). Inlet H₂S staircase step perturbations were studied using a feedforward control and the effect of EBRT considered by feedback control. The tuning method by maintained oscillation shows the lower errors. The selected controller was a PI, because unstable behavior at the lowest H₂S inlet loading was found under a PID controller. The PI control was able to maintain an outlet H₂S concentration of 14.7 ± 0.45 ppm_v at three EBRT, studied at 117 s, 92 s and 67 s. Therefore, desulfurized biogas could be used to feed a fuel cell. Feedforward control enhances BTF performance compared to the system without control. The maximum outlet H₂S concentration was reduced by 26.18%, although sulfur selectivity did not exceed 55%, as elemental sulfur was the main oxidation product.

Keywords: Anoxic; biogas desulphurization; feedback control; feedforward control; nitrite

1. Introduction

Control systems were initially developed in the chemical industry; however, it is easy to find several applications in bioprocess, combined with the development of data acquisition systems. These tools have allowed efficient monitoring of bioprocesses, contributing positively to the development of process-saving costs and guaranteeing the right conditions for the growth and maintenance of the microorganisms involved in these systems.

For biological processes, the most used control strategies are feedback and feedforward, depending on the specific characteristic of each system. In feedback controls, the controller calculates error as the difference between the measured controlled variable and the set point value. The controller applies an action into the system, based on the error value, to minimize its value. The main feedback control is a proportional-integral-derivative (PID) controller. The output of a PID controller can be calculated as follows [1]:

$$u(t) = k_p \cdot e(t) + \frac{k_p}{\tau_I} \int e(t) \cdot dt + k_p \cdot \tau_D \frac{de(t)}{dt} \quad (1)$$

where k_p is the proportional gain, τ_I is the integral time and τ_D is the derivative time.

In feedforward control, it is imperative to have thorough knowledge of the process. Variation in disturbance variable (inlet variable) is measured and the manipulated variable is adjusted to minimize deviations in the control variable using a mathematical model [2].

In feedback control, the most critical step is controller tuning [3], where the main parameters are estimated using mathematical equations or algorithms. Tuning methods are necessary when a control system is implemented or when deterioration in the control of a previously implemented system is observed. Importantly, tuning rules are based on the heuristic postulates of Ziegler and Nichols [4].

These rules have had a great influence on the implementation of Proportional Integral Derivative (PID)-type controllers for more than half a century [1]. However, other tuning methods have been developed (considering that several tuning rules can be used in the same system [5]) to improve the weakness of the Ziegler-Nichols rules due to characterization of a dynamic process from scarce information, possibly with little robustness and damping of the controlled variable. Therefore, other tuning methods have been developed, based on the rejection of load perturbations and noise measurement, sensitivity to modeling errors, and set point response [6].

Although feedback control is the most common strategy used in industrial processes owing to its simplicity, in some processes, this strategy cannot provide the required control due to time delays or the appearance of variables not foreseen in the system [7].

In this sense, feedforward control measures the disturbances and performs the compensation before the controlled variable deviates from the set point. However, the sensitivity to unpredictable disturbances is the most important limitation of feedforward control [8]. The principal applications for biological systems are related to the optimization of nutrient feeding (oxygen, substrate, etc.) [9,10] and preventing toxic compound accumulation in these systems [11]. In an anoxic biotrickling filter (BTF) for biogas desulfurization, feedforward control has been used in the regulation of the electron acceptor (nitrate) feeding according to the H_2S inlet load (IL) at constant biogas flow rate [12]. Moreover, the use of nitrite has shown good performance in an anoxic biotrickling filter for H_2S removal using feedback control [13]. The use of nitrite is interesting because the BTF could be coupled with a nitrification bioreactor [13,14].

The aim of the work described here was to use different tuning methods and study H_2S inlet perturbations using feedforward (inlet H_2S staircase step perturbation) and feedback (EBRT modifications) controls. EBRT is an operational variable that has been scarcely studied. In fact, most studies have been carried out with EBRT higher than that used in this study. The bioreactor was an anoxic BTF using nitrite as an electron acceptor to mimic biogas desulfurization.

2. Materials and Methods

2.1. BTF Set Up

The experimental work was done in a lab scale BTF operated in co-current gas flow mode. Therefore, the gas inlet was located at the top of the column, with the gas and liquid flowing in parallel. The trickling liquid velocity (TLV) was 10 m h^{-1} and mimic biogas (mixture of H_2S and balance to N_2) was fed to the system. The bioreactor was made of transparent PVC and packed with 5/8" Pall rings (Pall Ring Company, UK). The column had a height of 70 cm and internal diameter of 7.14 cm, with working volume of 2.8 L. The temperature was kept constant at 30°C by a cooling thermostat (Lauda, Germany) using a heater exchanger in the recirculation medium. pH was controlled at 7.4 using an ON/OFF control (Multimeter 44, Crison, Spain) on peristaltic pumps by automated addition of NaOH 5 M or H_3PO_4 0.66 M. The system was controlled and monitored using the LabVIEW™ platform (National Instruments™, USA) with cDAQ Chassis (NI-9184) with three modules: NI-9208 (current input module), NI-9264 (voltage output module) and NI-9375 (digital I/O module).

The mineral medium composition was (g L^{-1}) [15]: NH_4Cl (1.0), K_2HPO_4 (2.0), $\text{MgSO}_4 \cdot 7\text{H}_2\text{O}$ (0.8), NaHCO_3 (1.78) as carbon source, trace elements solution SL-4 (5 mL L^{-1}) and a solution of $\text{FeSO}_4 \cdot 7\text{H}_2\text{O}$ (2 g in 1 L H_2SO_4 0.1 N) (10 mL L^{-1}). The trace element solution (SL-4) composition was: EDTA (0.5 g L^{-1}), $\text{FeSO}_4 \cdot 7\text{H}_2\text{O}$ (0.2 g L^{-1}) and trace element solution SL-6 (100 mL L^{-1}). The composition of the trace element solution (SL-6) (g L^{-1}) was: $\text{ZnSO}_4 \cdot 7\text{H}_2\text{O}$ (0.1), $\text{MnCl}_2 \cdot 4\text{H}_2\text{O}$ (0.03), H_3BO_3 (0.3), $\text{CoCl}_2 \cdot 6\text{H}_2\text{O}$

(0.2), $\text{CuCl}_2 \cdot 2\text{H}_2\text{O}$ (0.01), $\text{NiCl}_2 \cdot 6\text{H}_2\text{O}$ (0.02), $\text{Na}_2\text{MoO}_4 \cdot \text{H}_2\text{O}$ (0.03). Sodium nitrite was used as an electron acceptor.

The outlet H_2S concentration was measured using an electrochemical sensor (SureCell, Euro-Gas Management Service, UK). Further information about the operation principle of the anoxic BTF can be found elsewhere [12,13,16].

2.2. Tuning of Feedback Control

Three methods for controller tuning were used—two of them based on Ziegler-Nichols rules (ZN) (step-response and maintained oscillation) and the third using the Approximate M-constrained Integral Gain Optimization (AMIGO). ZN (step-response) and AMIGO methods required a step inlet perturbation and system response, which was monitoring and recording—the inlet H_2S concentration was increased by 20% from 1900 to 2280 ppm_v (IL from 79.80 to 95.80 gS- H_2S m⁻³ h⁻¹) until the outlet H_2S concentration (control variable) was constant (steady state conditions). This increase in the inlet concentration is enough to observe the response of the system without reduction in the removal efficiency of the BTF; the usual critical elimination capacity in anoxic BTF is above 100 gS- H_2S m⁻³ h⁻¹ [17].

The graphical information obtained about the process from a step-response test in open loop was used to calculate the gain (K), delay time (L), and constant time (T). K corresponds with response increase, L and T were determined using the maximum slope tangent of the response curve [6]. Thus, the specific gain for each controller can be obtained by the mathematical equations shown in Table 1 [18,19].

Table 1. Tuning rule for the step response method.

Parameters	Ziegler-Nichols			AMIGO	
	PID	PI	P	PID	PI
Proportional gain (k_p)	$\frac{1.2T}{KL}$	$\frac{0.9T}{KL}$	$\frac{T}{KL}$	$\frac{0.2+0.45\frac{T}{L}}{K}$	$\frac{0.25T}{KL}$
Integral time (τ_I)	2L	3L	-	$0.4L + \frac{0.8T}{L+0.1T}$	0.8 T
Derivative time (τ_D)	L/2	-	-	$\frac{0.5LT}{0.3L+T}$	-

Integral (k_i) and derivative (k_d) gains can be calculated according to Equation (2) and Equation (3):

$$k_i = \frac{k_p}{\tau_I} \quad (2)$$

$$k_d = k_p \cdot \tau_D \quad (3)$$

Maintained oscillation (MO) tuning method, also known as frequency-response, is based on the fact that most processes have a stable monotonous response to a step input to the system [20]. Experimentally, the BTF was controlled by the action of proportional gain (P controller), at constant inlet H_2S concentration of 2280 ppm_v (IL of 95.80 gS- H_2S m⁻³ h⁻¹). Then, the value of the proportional gain was progressively increased from the initial value of 0.07, until the system becomes oscillatory and has continuous cycling (maintained oscillations). At that moment, it reaches the ultimate gain (K_U) and the ultimate period (P_U) of the oscillations. Thus, the specific parameters for each controller can be calculated using the mathematical equations shown in the Table 2 and Equation (2) and Equation (3) [21].

Table 2. Tuning rule for the maintained oscillation method.

Parameters	PID	PI	P
Proportional gain (k_p)	0.6 K_U	0.45 K_U	0.5 K_U
Integral time (τ_I)	0.5 P_U	0.85 P_U	-
Derivative time (τ_D)	0.125 P_U	-	-

2.3. Feedback Controller Selection

Once the gains were obtained for all the controllers adjusted by means of the three methods (ZN, MO and AMIGO), the most suitable one was selected based on the interpretation of Integral of Square of Errors (ISE), Integral of Absolute of Error (IAE), and Integral of Time multiplied Absolute of Errors (ITAE) [20]. For each controller, a step inlet perturbation was conducted, the inlet H₂S concentration was increased from 1900 to 2280 ppm_v, and the values of ISE, IEA and ITAE were calculated considering a time period of 60 min.

The two best gains set were selected to study their behavior under stair step perturbation. The EBRT was maintained at 117 s for 14 h. The H₂S IL was in the range of 28.1 to 141.1 gS-H₂S m⁻³ h⁻¹. This H₂S IL perturbation has been tested before for aerobic and anoxic BTFs [12,13,16] in a bid to simulate biogas from a wastewater treatment plant. The set point was 100 ppm_v.

2.4. Effect of EBRT Using a Feedback Controller

Three EBRT of 117 s, 92 s and 67 s were studied. For each EBRT, the inlet H₂S concentration profile was variable, according a discretized stair sinusoidal function every 0.5 h (Equation (4)).

$$H_2S_{in} = 410 \sin\left(\frac{2\pi}{24}t\right) + 590 \quad (4)$$

Therefore, the H₂S IL was between: 7–39, 9–50 and 12–69 gS-H₂S m⁻³ h⁻¹, for 117 s, 92 s and 67 s, respectively. The inlet H₂S concentration profile was between 180–1000 ppm_v during the course of 24 hours, according to typical values recorded in some waste treatment processes; for example in organic fraction of municipal solid waste [22]. The average inlet H₂S concentration was 590 ppm_v with amplitude oscillation of 410 ppm_v. The set point was maintained at 15 ppm_v, a value that allowed other biogas applications, such as fuel cells, to understand the behavior of the control system [23,24].

2.5. Feedforward Control

A detailed description of the control system used in this study has been previously described by López et al. [12]. Two similar experiments at EBRT of 117 s with and without control were carried out to make a corresponding comparison using a variable profile of the H₂S IL for 14 h between 28.10–141.10 gS-H₂S m⁻³ h⁻¹ (710 – 3564 ppm_v), which covers real fluctuations that can be found in industrial installations [25]. The average H₂S IL was of 79.80 gS-H₂S m⁻³ h⁻¹.

For the experiment with control, a molar ratio N:S_{in} of 1.3 mol-N mol-S⁻¹ was selected, increasing the nitrite supply by 62% regarding experiments with nitrate [12]. To maintain this value, the flow rate of the nitrite feeding pump was between 0.10–0.49 L h⁻¹. In contrast, for the experiment without control, the nitrite concentration in the dosing tank and the inlet flow rate were kept constant at 0.46 gN-NO₂⁻ L⁻¹ and 0.28 L h⁻¹, respectively. Therefore, the molar ratio N:S was variable between 0.74 and 3.70 mol-N mol-S⁻¹.

3. Results and Discussion

3.1. Tuning

The system response observed in the outlet H₂S concentration is shown in Figure 1, for maintained oscillation (Figure 1a) and step response (Figure 1b) methods.

According to the MO method, the ultimate gain (K_U) was 0.14 and ultimate period (P_U) was 148 s. The K_U was ten time higher than the value obtained using nitrate (K_U = 0.015) and the P_U was almost half the value obtained using nitrate (P_U = 343 s) [16]. Thus, a lower value of P_U produced an increase in the integral gain with a stabilizing effect on the oscillations during the response of the control variable [26]. On the other hand, an increase of the K_U value increases all the gains (proportional, integral and derivative), which, may have a delayed effect on the control. However, these correlations

may not be accurate, because the gains are dependent on each other and the change in one of them may produce changes in the effect of the other two [26]. The K_U and P_U allowed to calculate the specific controller gains, which are shown in Table 3.

Moreover, the graphical procedure for the step-response method is represented in Figure 1b. After the step perturbation, the outlet H_2S concentration increased from 66.7 to 138.6 ppm_V (RE 94.0%). Therefore, the H_2S concentration versus time allowed to obtain gain (K), delay time (L) and constant time (T), parameters that were used in the gain's calculation (Table 3).

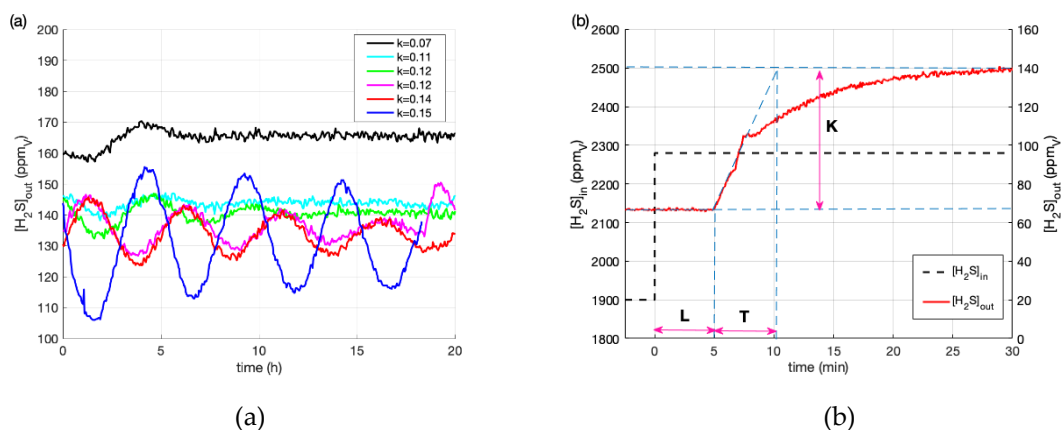


Figure 1. Controller tuning: (a) maintained oscillation method. Outlet H_2S concentration versus time at several proportional gains; (b) step-response method (Ziegler-Nichols rules (ZN)). Inlet and outlet H_2S concentration versus time.

Table 3. Gains for step-response and maintained oscillation methods.

Gains	Ziegler-Nichols			AMIGO		Maintained oscillation		
	PID	PI	P	PID	PI	PID	PI	P
k_p	1.75×10^{-2}	1.31×10^{-2}	1.46×10^{-2}	9.34×10^{-3}	3.64×10^{-3}	8.40×10^{-2}	6.3×10^{-2}	7.00×10^{-2}
k_i	9.45×10^{-6}	4.73×10^{-6}	-	8.71×10^{-6}	4.70×10^{-6}	1.14×10^{-3}	5.11×10^{-4}	-
k_d	8.09	-	-	3.36	-	1.55	-	-

A comparison of the calculated gains (Table 3) by ZN and AMIGO with the values obtained by tuning during the nitrate operation [16] showed significant variation. Specifically, the proportional and integral gains for the PID and PI controllers showed a variation of 76.37 – 98.11%, while in the derivative gain, values observed an increase of 141.34 – 145.01%. However, the marked difference between the obtained parameters did not have a negative influence on the process control, despite previously being described in literature, where gain values variations lower than 50% rarely have significant effects on the response of the feedback control system [26]. Therefore, a system can not only be controlled with different gain values, but also with significantly different values found in the others.

3.2. Controller Selection

Same step perturbation was evaluated for each PI and PID controller (Figure 2), monitoring the signal response (Figure 2a) of the control variable (H_2S_{out}) for 1 h. Thus, the graphical signal record was used for error calculation (IAE, ISE and ITAE) (Table 4), in order to select the appropriate controller with the lowest error criteria [2].

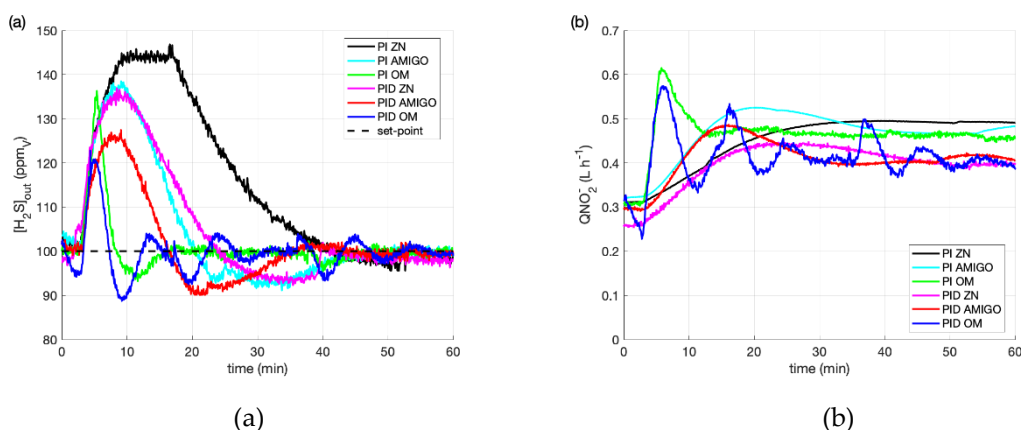


Figure 2. Controller selection: (a) outlet H_2S concentration for PI and PID controllers; (b) nitrate flow rate (controlled variable) for PI and PID controllers.

Table 4. Integral errors for PI and PID controllers.

Errors	Ziegler-Nichols		AMIGO		Maintained oscillation	
	PID	PI	PID	PI	PID	PI
ISE	233.1	559.5	110.7	255.5	28.0	32.1
IAE	9.9	16.0	6.8	10.4	3.2	2.7
ITAE	170.9	274.3	118.5	117.8	58.5	45.8

However, while recording the nitrite inlet flow (Figure 2b) for each controller, it is important to remark the oscillatory response observed in the manipulated variable for the PID-MO respect to the other controllers. Thus, an unstable system is expected with this behavior, maintained or increased over time. A comparison of the calculated errors (Table 4) indicates a significant reduction between the errors calculated for the PI and PID controllers tuned by MO, respect to the step-response tuning.

Table 5 shows the offset, stabilization time (time until setpoint is reached), and average, maximum and minimum outlet H_2S concentration. The offsets, average, maximum and minimum H_2S concentrations were similar in the six controllers; likewise, the lower stabilization time was for the PI and PID control tuned by the MO method.

Table 5. Comparison of controller response.

	Ziegler-Nichols		AMIGO		Maintained oscillation	
	PID	PI	PID	PI	PID	PI
Offset (ppmV)	3.05	3.65	2.16	2.17	2.73	4.03
Stabilization time (h)	0.66	0.84	0.65	0.73	0.46	0.28
$[H_2S]_{average}$ (ppmV)	98.9	99.2	99.9	99.7	99.6	99.5
$[H_2S]_{min} - [H_2S]_{max}$ (ppmV)	96.9–102.0	95.5–101.8	97.7–102.1	97.5–101.5	96.8–101.5	95.4–102.3

In general, the errors calculated in nitrite operation are higher than those calculated in nitrate operation [27], probably because of an increase of sensitivity in nitrite operation. In relation with stabilization time, a similar value of 0.41 was obtained by Brito et al. [16] using nitrate and PID controller tuned by MO.

As a comparative result, PID-MO and PI-MO were selected to evaluate a variable H_2S IL profile (Figure 3), controlling the H_2S outlet concentration at a set point of 100 ppmV.

Under the action of the PID-MO controller (Figure 3a), the system became unstable at the lowest value of the studied H_2S IL profile. The amplitude of the observed oscillations in nitrite flowrate

increase as the IL decrease (lower range 28.10 – 56.30 gS-H₂S m⁻³ h⁻¹), while the system recovered the control action at the higher values of the H₂S IL profile studied.

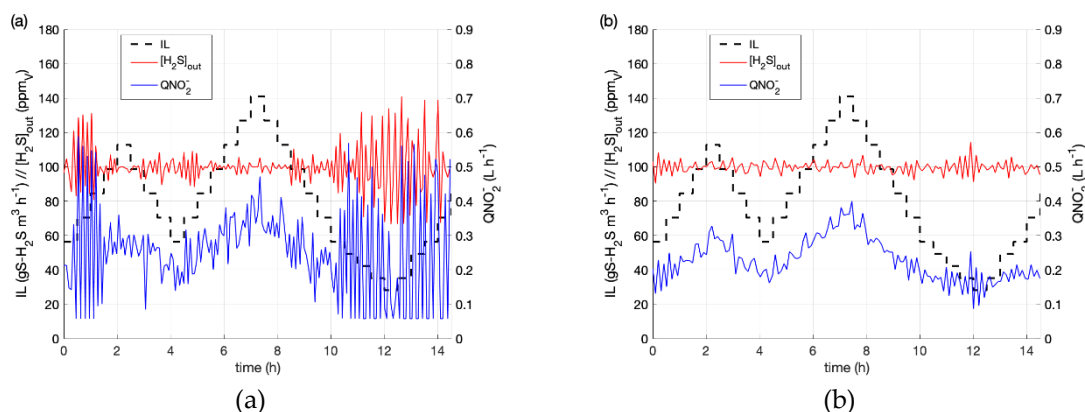


Figure 3. Staircase perturbation for PID (a) and PI (b) adjusted by MO. Blue lines: nitrite flowrate, red lines: H₂S_{out}, dashed black lines H₂S IL.

However, a completely different pattern was observed under the PI-MO controller (Figure 3b), where the control variable was satisfactory controlled between 90.40 – 114.30 ppm_V along the full staircase analyzed profile. Therefore, the PI-MO controller was selected to carry out the study of the control system to changes in the EBRT.

Thus, the selection criteria based on integral time can be accepted for controller selection; nevertheless, it is not a definitive criterion, as the above results show. The cause, probably, could be in the tuning process of the controllers and the influence of other disturbances, which was randomly present during data acquisition, which is subsequently used in the error calculation.

The stability of the system is more important than the fluctuations in the outlet H₂S concentration. It is, therefore, desirable to have a low fluctuation of nitrite flow rate, even if this means a fluctuation of the outlet H₂S concentration. Biogas desulfurization by an anoxic BTF using a nitrification reactor compared to the use of commercial nitrate reduces its environmental impact (61.4%) and bring operational cost down—from 6.31 to 4.34 € per kg of S-H₂S treated [28]. In addition, it is necessary to avoid fluctuations in nitrite flow rate, as these would involve hydraulic residence time fluctuations in the nitrification bioreactor, which could affect its performance [29]. The feasibility of coupling both bioreactors, nitrification and BTF, has been proven at pilot plant [30]. Thus, the use of a PI control system adjusted by the MO method has two important advantages: good adjustment of the outlet H₂S concentration and low fluctuation of the nitrite flow rate.

3.3. EBRT Study under Feedback Control

With the selected controller (PI-MO), the influence of EBRT on the control of the H₂S outlet concentration at a set point of 15 ppm_V was studied. Figure 4 shows the performance of the outlet H₂S concentration (Figure 4a) and of the nitrite flow rate (Figure 4b) for the three EBRT studies (117, 92 and 67 s).

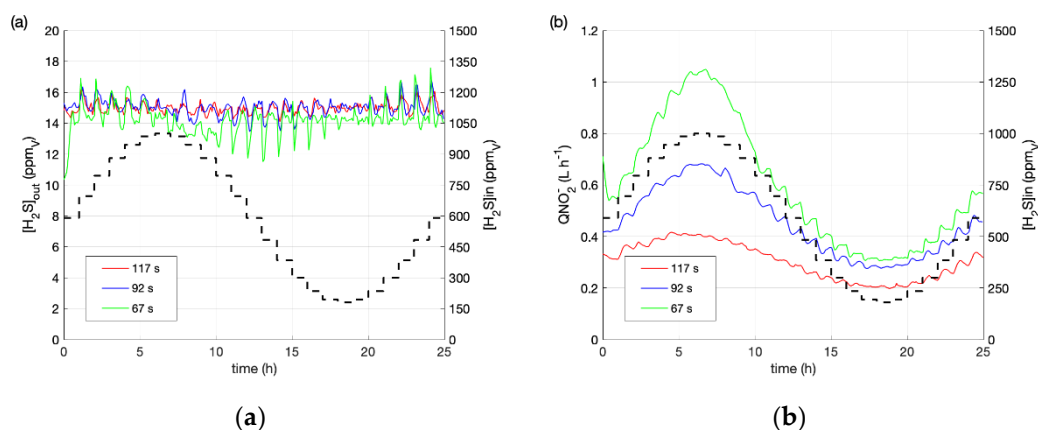


Figure 4. Profiles obtained in EBRT studies at 67 s, 92 s and 117 s. **(a)** H_2S outlet concentration, **(b)** nitrite flowrate. Green lines: 67 s; blue lines: 92 s; red lines: 117 s; dashed black lines: $\text{H}_2\text{S}_{\text{in}}$.

The PI-MO controller was able to adjust the control variable at 117 s and 92 s in $14.98 \pm 0.37 \text{ ppm}_V$ and 15.00 ± 0.56 , respectively, while at the lowest EBRT tested, the adjustment of the $\text{H}_2\text{S}_{\text{out}}$ concentration was shifted up to $14.21 \pm 0.98 \text{ ppm}_V$.

As a consequence of the control action, the variation in the nitrite flow rate was significant among the three EBRT analyzed (Figure 4b), specially at high values of the studied profile (500–1000 ppm_V). Thus, the nitrite flow rate of 117 s was incremented by 50.88% ($0.13 - 0.32 \text{ g N-NO}_2^- \text{ h}^{-1}$) and 96.13% ($0.14 - 0.48 \text{ g N-NO}_2^- \text{ h}^{-1}$) for EBRT of 92 s and 67 s, respectively. For the three EBRT studied, the low output concentration of H_2S allowed other uses of the treated biogas, as it could be fuel cells [23,24].

The H_2S IL were between: 7–39, 9–50 and 12–69 $\text{gS-H}_2\text{S m}^{-3} \text{ h}^{-1}$, for 117 s, 92 s and 67 s, respectively. Previous studies have usually been carried out at H_2S IL higher than $100 \text{ gS-H}_2\text{S m}^{-3} \text{ h}^{-1}$ [12,16,31] because it has been used to treat biogas with high H_2S concentrations, such as the biogas produced in a waste water treatment plant (WWTP) [32]. However, it is possible to find biogas with lower H_2S concentrations, such as landfill biogas, which has H_2S concentration in the range studied in this section (between 180–1000 ppm_V) [24]. Thus, with landfill biogas, a lower EBRT could be used, allowing to obtain an outlet H_2S concentration of above 15 ppm_V , which would offer more profitable biogas applications than burning in a cogeneration engine. Moreover, a lowest EBRT reduces the size of the package and therefore the installation cost [33]. In addition, the presence of leachate in landfills and ammonium-rich effluents could be used to biologically produce nitrites [34]. As far as we know, this study has tested the lowest EBRT on anoxic BTFs; EBRTs are usually larger (342 s [14], 321 s [35], 176 s [36] or 117 s [16]).

3.4. Effects of Feedforward Control Strategy on the Outlet H_2S Concentration and Sulfate Selectivity

Figure 5 shows the outlet H_2S concentration (Figure 5a) and inlet molar ratio N:S (Figure 5b) for experiments with and without feedforward control for the stair's sinusoidal perturbation on H_2S IL.

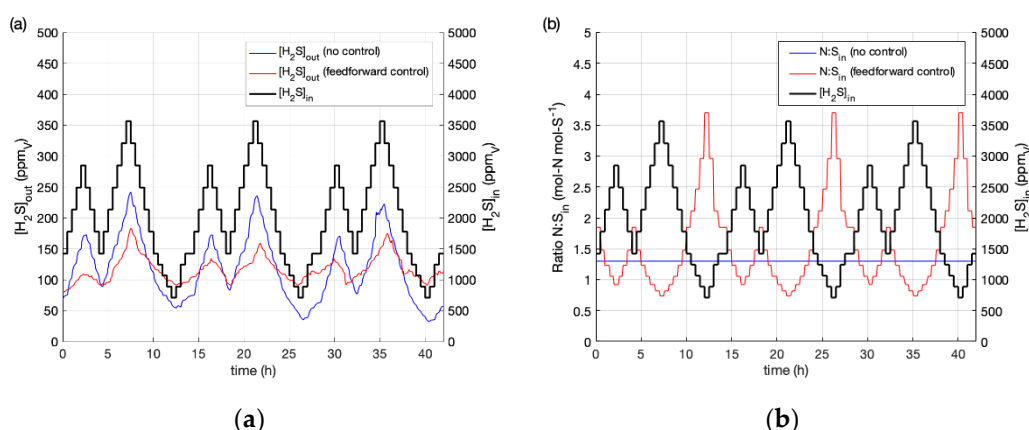


Figure 5. Profiles along experimental tests. (a) $\text{H}_2\text{S}_{\text{out}}$ concentration. (b) Inlet molar ratio $\text{N}:\text{S}_{\text{in}}$. Blue lines: controlled experiments; dashed black lines: $\text{H}_2\text{S}_{\text{in}}$; red lines: experiments without control.

An improvement on the BTF operation was observed using the feedforward control, with respect to the experiment without control (Figure 5a). The maximum output H_2S concentration was reduced by 26.18%, since in the experiment without control, the maximum outlet H_2S concentration reached was 233 ppm_V and 172 ppm_V for the feedforward control with an average of 117 ± 21 ppm_V, corresponding to an elimination percentage of 93 ± 2 %. Moreover, the emitted mass of the system (gS- H_2S) was reduced by 2.6% (from 0.18 gS- H_2S to 0.15 gS- H_2S). Therefore, the results were similar to a study previously done using nitrate as an electron acceptor [12]. The possibility of using nitrite instead of nitrate is very interesting, as it can reduce the production cost in a nitrification reactor due to the lower energy consumption in the air supply [37].

For both experiments, feedforward and without control, elemental sulfur was the main oxidation product. The average values were 0.25 ± 0.14 and 0.22 ± 0.01 gS- SO_4^{2-} (gS- $\text{H}_2\text{S}_{\text{removed}}$)⁻¹ for the experiment without and with feedforward control. Although during the experiment without control in the lowest H_2S IL (35.2 to 28.1 gS- H_2S m⁻³ h⁻¹), the inlet molar ratio $\text{N}:\text{S}$ exceeded the theoretical value for 100% of sulfate production (2.6 mol-N- NO_2^- -mol-S⁻¹ [38]); the sulfate selectivity never exceeded 55%. These results could be due to the fact that sulfur oxidation occurs in two stages and probably elemental sulfur may not oxidize until the sulfide present in the system has been exhausted [39]. Using nitrate [12], a higher sulfate selectivity was obtained, which could be related to structural changes in the microbial population [13].

4. Conclusions

The best tuning method was the maintained oscillation with the lowest error values (IAE, ISE and ITAE) in the specific response, compared to the rest of tuned controllers. However, PID-MO showed unstable control at low H_2S IL of the tested profile. The anoxic BTF under PI-MO controller action was able to work at low EBRT (from 117 s down to 67 s), with outlet H_2S concentration below 15 ppm_V, which extends the use of biogas for a more profitable approach, such as fuel cell, rather than burning in an engine system. This work also showed the usefulness of feedforward control for nitrite dosage in anoxic BTF, even at a varying H_2S IL profile (extremely changing conditions). In addition, this control strategy allowed to reduce H_2S outlet concentration peaks and the emitted H_2S mass by 26.18% and 2.6%, respectively.

Author Contributions: Research design, F.A., M.R. and D.C.; methodology, F.A. and M.R.; investigation, J.B. and F.A.; writing—original draft preparation, J.B.; writing—review and editing, M.R.; supervision, D.C. and M.R.; funding acquisition, D.C. and M.R.

Funding: This research was funded by “Ministerio de Economía y Competitividad”, grant number CTM2012-37927-C03/FEDER “Monitoring, modelling and control towards the optimization of anoxic and aerobic desulfurizing biotrickling”.

Conflicts of Interest: The authors declare no conflict of interest.

References

1. Åström, K. *Control System Design Lecture Notes for ME 155A*; Department of Automatic Control Lund Institute of Technology: Lund, Sweden, 2002; p. 333.
2. Poe, W.A.; Mokhtab, S. Chapter 3 Process Control. In *Modeling, Control, and Optimization of Natural Gas Processing Plants*; Elsevier Inc.: Amsterdam, The Netherlands, 2017; pp. 97–172, ISBN 9780128029619.
3. Rajinikanth, V.; Latha, K. Identification and Control of Unstable Biochemical Reactor. *Int. J. Chem. Eng. Appl.* **2010**, *1*, 106–111. [[CrossRef](#)]
4. Visioli, A. Fuzzy logic based set-point weight tuning of PID controllers. *IEEE Trans. Syst. ManCybern. Part A Syst. Hum.* **1999**, *29*, 587–592. [[CrossRef](#)]
5. Yu, C.-C. *Autotuning for PID Controllers. Relay Feedback Approach*; Springer: Berlin, Germany, 1999; ISBN 9781447136385.
6. Åström, K.; Hägglund, T. *PID Controllers: Theory, Design, and Tuning*; Instrument Society of America: Pittsburgh, PA, USA, 1995; ISBN 1556175167.
7. Svrcek, W.Y.; Mahoney, D.P.; Young, B.R. *A Real-Time Approach to Process Control*, 2nd ed.; John Wiley & Sons Ltd.: Chichester, England, 2006; ISBN 978-0-470-02533-8.
8. Cervin, A.; Eker, J.; Bernhardsson, B.; Årzén, K.-E. Feedback–Feedforward Scheduling of Control Tasks. *Real Time Syst.* **2002**, *23*, 25–53. [[CrossRef](#)]
9. Rieger, L.; Jones, R.M.; Dold, P.L.; Bott, C.B. Ammonia-Based Feedforward and Feedback Aeration Control in Activated Sludge Processes. *Water Environ. Res.* **2014**, *86*, 63–73. [[CrossRef](#)] [[PubMed](#)]
10. Versyck, K.J.; Van Impe, J.F. Optimal design of a closed loop controller for estimation of parameter couples of microbial growth kinetics. *Chem. Eng. Commun.* **2000**, *180*, 39–59. [[CrossRef](#)]
11. Zhao, H.; Isaacs, S.H.; Søeberg, H.; Kümmel, M. A novel control strategy for improved nitrogen removal in an alternating activated sludge process—Part II. Control development. *Water Res.* **1994**, *28*, 535–542. [[CrossRef](#)]
12. López, L.R.; Brito, J.; Mora, M.; Almenglo, F.; Baeza, J.A.; Ramírez, M.; Lafuente, J.; Cantero, D.; Gabriel, D. Feedforward control application in aerobic and anoxic biotrickling filters for H₂S removal from biogas. *J. Chem. Technol. Biotechnol.* **2018**, *93*, 2307–2315. [[CrossRef](#)]
13. Brito, J.; Valle, A.; Almenglo, F.; Ramírez, M.; Cantero, D. Progressive change from nitrate to nitrite as the electron acceptor for the oxidation of H₂S under feedback control in an anoxic biotrickling filter. *Biochem. Eng. J.* **2018**, *139*, 154–161. [[CrossRef](#)]
14. Zeng, Y.; Luo, Y.; Huan, C.; Shuai, Y.; Liu, Y.; Xu, L.; Ji, G.; Yan, Z. Anoxic biodesulfurization using biogas digestion slurry in biotrickling filters. *J. Clean. Prod.* **2019**, *224*, 88–99. [[CrossRef](#)]
15. Fernández, M.; Ramírez, M.; Pérez, R.; Gómez, J.; Cantero, D. Hydrogen sulphide removal from biogas by an anoxic biotrickling filter packed with Pall rings. *Chem. Eng. J.* **2013**, *225*, 456–463. [[CrossRef](#)]
16. Brito, J.; Almenglo, F.; Ramírez, M.; Gómez, J.M.; Cantero, D. PID control system for biogas desulfurization under anoxic conditions. *J. Chem. Technol. Biotechnol.* **2017**, *92*, 2369–2375. [[CrossRef](#)]
17. Montebello, A.M.; Fernández, M.; Almenglo, F.; Ramírez, M.; Cantero, D.; Baeza, M.; Gabriel, D. Simultaneous methylmercaptan and hydrogen sulfide removal in the desulfurization of biogas in aerobic and anoxic biotrickling filters. *Chem. Eng. J.* **2012**, *200–202*, 237–246. [[CrossRef](#)]
18. Åström, K.J.; Hägglund, T. Revisiting the Ziegler–Nichols step response method for PID control. *J. Process Control* **2004**, *14*, 635–650. [[CrossRef](#)]
19. Hägglund, T.; Åström, K. Revisiting the Ziegler–Nichols Tuning Rules for Pi Control. *Asian J. Control* **2002**, *4*, 364–380. [[CrossRef](#)]
20. Cominos, P.; Munro, N. PID controllers: Recent tuning methods and design to specification. *IEEE Proc. Control Theory Appl.* **2002**, *149*, 46–53. [[CrossRef](#)]
21. Hang, C.; Åström, K.; Ho, W. Refinements of the Ziegler–Nichols tuning formula. *IEEE Proc. D Control Theory Appl.* **1991**, *138*, 111. [[CrossRef](#)]
22. Papurello, D.; Soukoulis, C.; Schuhfried, E.; Cappellin, L.; Gasperi, F.; Silvestri, S.; Santarelli, M.; Biasioli, F. Monitoring of volatile compound emissions during dry anaerobic digestion of the Organic Fraction of Municipal Solid Waste by Proton Transfer Reaction Time-of-Flight Mass Spectrometry. *Bioresour. Technol.* **2012**, *126*, 254–265. [[CrossRef](#)]

23. Papurello, D.; Borchellini, R.; Bareschino, P.; Chiodo, V.; Freni, S.; Lanzini, A.; Pepe, F.; Ortigoza, G.A.; Santarelli, M. Performance of a Solid Oxide Fuel Cell short-stack with biogas feeding. *Appl. Energy* **2014**, *125*, 254–263. [[CrossRef](#)]
24. Ramírez, M.; Gómez, J.; Cantero, D.; Ramírez, M.; Gómez, J.; Cantero, D. *Biogas: Sources, Purification and Uses; Hydrogen and Other Technologies*; Studium Press LLC: Daryaganj, India, 2015; Volume 11, pp. 296–323, ISBN 978-1-626990-72-2.
25. Gabriel, D.; Deshusses, M.A.; Gamisans, X. Desulfurization of Biogas in Biotrickling Filters. In *Air Pollution Prevention and Control: Bioreactors and Bioenergy*; John Wiley & Sons, Ltd.: Chichester, UK; Hoboken, NJ, USA, 2013; pp. 513–523, ISBN 9781118523360.
26. Smith, C.A.; Corripio, A. *Principles and Practice of Automatic Process Control*, 3rd ed.; John Wiley & Sons Inc.: Hoboken, NJ, USA, 2005; ISBN 0471431907.
27. Brito, J. Diseño e Implementación de Estrategias de Control en un Biofiltro Percolador Anóxico Para la Desulfuración de Biogás. Ph.D. Thesis, University of Cádiz, Cádiz, Spain, 2017.
28. Cano, P.I.; Colón, J.; Ramírez, M.; Lafuente, J.; Gabriel, D.; Cantero, D. Life cycle assessment of different physical-chemical and biological technologies for biogas desulfurization in sewage treatment plants. *J. Clean. Prod.* **2018**, *181*, 663–674. [[CrossRef](#)]
29. Dinçer, A.R.; Kargi, F. Effects of operating parameters on performances of nitrification and denitrification processes. *Bioprocess Eng.* **2000**, *23*, 75–80. [[CrossRef](#)]
30. Zeng, Y.; Xiao, L.; Zhang, X.; Zhou, J.; Ji, G.; Schroeder, S.; Liu, G.; Yan, Z. Biogas desulfurization under anoxic conditions using synthetic wastewater and biogas slurry. *Int. Biodeterior. Biodegrad.* **2018**, *33*, 247–255. [[CrossRef](#)]
31. Cano, P.I.; Brito, J.; Almenglo, F.; Ramírez, M.; Gómez, J.M.; Cantero, D. Influence of trickling liquid velocity, low molar ratio of nitrogen/sulfur and gas-liquid flow pattern in anoxic biotrickling filters for biogas desulfurization. *Biochem. Eng. J.* **2019**, *148*, 205–213. [[CrossRef](#)]
32. López, L.; Dorado, A.; Mora, M.; Gamisans, X.; Lafuente, J.; Gabriel, D. Modeling an aerobic biotrickling filter for biogas desulfurization through a multi-step oxidation mechanism. *Chem. Eng. J.* **2016**, *294*, 447–457. [[CrossRef](#)]
33. Lebrero, R.; Gondim, A.; Pérez, R.; García-Encina, P.A.; Muñoz, R. Comparative assessment of a biofilter, a biotrickling filter and a hollow fiber membrane bioreactor for odor treatment in wastewater treatment plants. *Water Res.* **2014**, *49*, 339–350. [[CrossRef](#)] [[PubMed](#)]
34. Miao, L.; Yang, G.; Tao, T.; Peng, Y. Recent advances in nitrogen removal from landfill leachate using biological treatments—A review. *J. Environ. Manag.* **2019**, *235*, 178–185. [[CrossRef](#)] [[PubMed](#)]
35. Soreanu, G.; Béland, M.; Falletta, P.; Ventresca, B.; Seto, P. Evaluation of different packing media for anoxic H₂S control in biogas. *Environ. Technol.* **2009**, *30*, 1249–1259. [[CrossRef](#)] [[PubMed](#)]
36. Almenglo, F.; Ramírez, M.; Gómez, J.; Cantero, D. Operational conditions for start-up and nitrate-feeding in an anoxic biotrickling filtration process at pilot scale. *Chem. Eng. J.* **2016**, *285*, 83–91. [[CrossRef](#)]
37. Zhou, X.; Zhang, X.; Zhang, Z.; Liu, Y. Full nitrification-denitrification versus partial nitrification-denitrification-anammox for treating high-strength ammonium-rich organic wastewater. *Bioresour. Technol.* **2018**, *261*, 379–384. [[CrossRef](#)]
38. Mahmood, Q.; Zheng, P.; Cai, J.; Wu, D.; Hu, B.; Li, J. Anoxic sulfide biooxidation using nitrite as electron acceptor. *J. Hazard. Mater.* **2007**, *147*, 249–256. [[CrossRef](#)]
39. Mora, M.; Fernandez, M.; Gomez, J.; Cantero, D.; Lafuente, J.; Gamisans, X.; Gabriel, D. Kinetic and stoichiometric characterization of anoxic sulfide oxidation by SO-NR mixed cultures from anoxic biotrickling filters. *Appl. Microbiol. Biotechnol.* **2015**, *99*, 77–87. [[CrossRef](#)]

